The geometry of visual signalling in a bird-of-paradise

Yseult Héjja-Brichard[1, 2]*, Thomas MacGillavry[1]*, Leonida Fusani[1, 2]

[1]*Department of Interdisciplinary Life Sciences, KLIVV, University of Veterinary Medicine, Vienna, Austria*
[2]*Department of Behavioural and Cognitive Biology, University of Vienna, Austria*
*Equal contribution and corresponding authors

Email for correspondence:
Y.H-B., yseulthb@gmail.com
T.M., macgillavry.thomas@gmail.com

Abstract

Effective visual signalling in animals requires an appropriate viewing geometry, which depends on both the visual system of signal receivers and the spatial context in which the signal is viewed. For example, visual acuity determines the distance at which fine-scale patterns can be resolved, while the visual field defines the space around the audience open to influence from visual signals, particularly when viewing displays at close range and from a predictable location and direction. During courtship, male Victoria's riflebirds (*Ptiloris victoriae*) perform two distinct displays: the circular-wings pose at a distance and the alternate wing-clap display at close range. Using avian vision modelling, we show that the circular-wings pose enhances detectability by producing a highly circular, optical "black hole" against the rainforest background when viewed from afar. When females approach the display perch, males switch to alternating movements of the wings at a short distance from the female's eyes, intermittently occluding ~60% of her visual field and thereby generating a dynamic visual background that likely accentuates flashing colour patches. Thus, black feather-morphing displays are highly detectable at long range and shift to function primarily as a visual background at close range. Our findings illustrate how different components of a courtship phenotype can be repurposed across viewing contexts to form an integrated signalling system in which signal efficacy is modulated by the spatial context in which the display is viewed.

Keywords: signal evolution, sexual selection, courtship, sensory ecology, display behaviour.

Introduction

For effective visual communication, a signal must not only exhibit salient colours and brightness, but also be produced in the appropriate viewing distance, direction, and position relative to the receiver's eyes (Endler et al. 2010; Yorzinski et al. 2013; Endler et al. 2014; Echeverri et al. 2021). This is especially relevant during sexual signalling, where receivers often view display behaviour from a predictable orientation and direction (Endler et al. 2010; Echeverri et al. 2017; Echeverri et al. 2021). Although much attention has been given to the evolution of colouration in visual signals (Cuthill et al. 2017), relatively little remains known about how geometric features of visual signals (e.g., effects related to position and orientation) determine efficacy from the audience's perspective (see Endler et al. 2010; Kelley and Endler 2012; Yorzinski et al. 2013; Endler et al. 2014). For instance, the eye's spatial resolution (i.e. visual acuity) may constrain the perception of finer-scale patterns at distance (Caves et al. 2018; Fleishman et al. 2020), while the field of view (FOV) shapes how displays are perceived up close (Endler et al. 2010; Endler et al. 2014; Echeverri et al. 2021), creating the potential for attention-capturing visual effects, including illusions (Endler et al. 2010; Santacà et al. 2025).

For example, male *Anolis* lizards display their colourful dewlaps across a range of spatial contexts, where limited visual acuity — especially in peripheral vision — causes fine-scale colour patterns to become resolvable only at close range or when they are performed in the receiver's fovea (Fleishman et al. 2017; Fleishman et al. 2020). In great bowerbirds (*Chlamydera nuchalis*), females watch male displays from a consistent position inside an avenue bower which restricts their FOV, allowing males to control the content and timing of

what they can see (Endler et al. 2010; Kelley and Endler 2012; Endler et al. 2014; MacGillavry et al. 2025). The context in which a visual signal is viewed is therefore of substantial importance for signal efficacy (Echeverri et al. 2021). Understanding how viewing context shapes signal perception is thus critical to decipher the design features of complex sexual displays.

Male birds-of-paradise (Aves: Paradisaeidae) perform some of the most elaborate sexual displays among birds (Scholes and Laman 2012). In some species, such as Victoria's riflebird (*Ptiloris victoriae*), males display solitarily atop vertical display posts in the rainforest understorey (Frith and Cooper 1996). When a female is within viewing distance, males perform an intricate "circular-wings display" pose in which both wings are raised with the wrists hyper-extended, forming a strikingly black, circular shape (Frith and Cooper 1996; MacGillavry et al. 2024). During this display, males maintain a consistent angle relative to females by tracking their movements (**Video S1**), only performing the dynamic "alternating wing-clap display" when a female visits the display site at close range (**Video S2**) (Frith and Cooper 1996; MacGillavry et al. 2025). Females appear to base their mating decisions on maximal display tempi of male mating dances, which consist of alternating motions with the wings and a small, blue plumage patch or yellow mouth integument (MacGillavry et al. 2025). The different display behaviours exhibited by male riflebirds are therefore linked to different viewing contexts: one performed at a distance and the other at close range. This means that different display behaviours are associated with highly distinct viewing geometries.

Although the temporal and rhythmic structure of this display is now known in detail (MacGillavry et al. 2025), its visual effects from the receiver's perspective remain unclear. One key feature is the extremely black plumage of adult males, which has been suggested to create the illusion of self-luminosity of colour patches, as the lack of specular highlights in black plumage curtails the visual system's capacity for colour constancy (McCoy et al. 2018). However, this mechanism alone does not provide a clear explanation for elaborate, black feather-morphing poses with rounded edges (see MacGillavry et al. 2024; MacGillavry 2025), which are not shared across all species with super-black plumage (McCoy et al. 2018; McCoy and Prum 2019). We thus hypothesised that black plumage, in conjunction with this characteristic circular shape, may also function to enhance contrast with the rainforest background when viewed from a distance, creating a conspicuous silhouette.

To examine how the feather morphing poses of male riflebirds appear to females within their ecological context, we used avian vision models to analyse images of displaying males collected in their natural environment. As colour calibration could not be obtained, images were greyscaled and filtered to simulate the female's visual perspective across a range of viewing distances in which females may be displayed to under natural conditions (**Figure 1**). We then compared the visual signal efficacy of adult male display poses to those of immature males, which perform the same species-typical display repertoire, but lack the characteristic super-black plumage. Finally, we further quantified geometric and fine-scale temporal features of the dynamic phase of display to elucidate the female's perspective at close range.

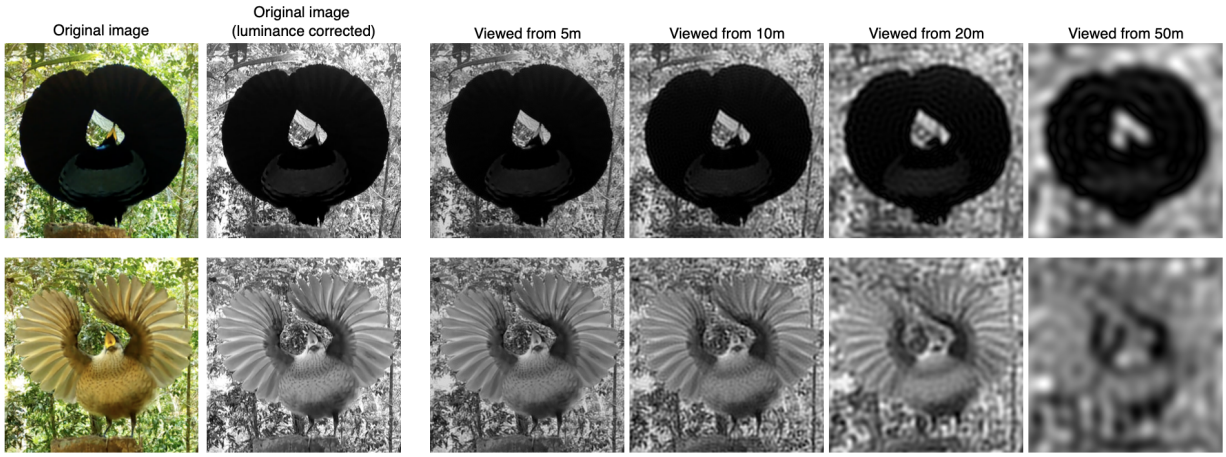

Figure 1. Riflebird display poses create a conspicuous "black hole" effect when viewed at a distance. Images show super-black adult (top row) and brown immature (bottom row) males. Original images were greyscaled and corrected for luminance before applying a low-pass filter to simulate a female riflebird's perception at different distances.

Materials & Methods

Study species, image collection, and image selection

Display behaviours of Victoria's riflebird (*Ptiloris victoriae*) were recorded in upland rainforest in the Atherton Tablelands in Queensland, Australia (17˚, 15', 55" S, 145˚, 37', 47" E) using motion-triggered trail cameras (Browning Recon Force Advantage HD; Browning Recon Force Elite HP5). Trail cameras were each installed as close as possible to the display perches by mounting them on the surrounding vegetation as level as possible to the top of the perch. Where possible, distances to the display perch were recorded using photographs, including a 1m ruler for reference and each camera was calibrated with a checkerboard pattern held perpendicular to the sensor. Video frames where males displayed the circular-wings pose approximately perpendicular to the camera sensor, with wings as fully raised as possible were selected (N = 7 adults and N = 6 immature males).

Bird banding was conducted with the approval of the Australian Bird and Bat Banding Scheme (R-class banding authority number: 3662; ABBBS project number: 3662-01). Ethical approval was granted by the Animal Ethics Committee of the Department of Agriculture and Fisheries (AEC reference number: CA 2022/02/1589). Field activities on freehold land (Center for Rainforest Studies; 17.283°S, 145.625°E) and at the Crater Lakes National Park (17.283°S, 145.625°E) were approved by the Queensland Wildlife and Parks Service (P-PTUKI-100257238; WA0045747). Video footage from trail cameras was sampled for frames in which displaying males performing the *circular-wings* pose were approximately perpendicular to the camera sensor, with wings as fully raised as possible. In total, we selected the best frames of 7 adult, and 6 immature *circular-wings* pose displays. All adult bird images come from different display perches, and immature bird images come from four different perches but at different times of the day thereby keeping variation in light intensity. Specific dates and times are reported in the image metadata file available in the GitHub repository of the project.

Image processing and analysis

Given the relatively unpredictable occurrence of riflebird displays and the use of camera traps, colour calibration for images of displaying birds at given times was not feasible and camera spectral sensitivities were not unavailable (i.e., no RAW or spectral images could be obtained). Therefore, we did not attempt to estimate avian cone catches and chose to generate an approximate achromatic representation of the scene by computing a weighted sum of RGB channels intended to mimic the broad medium-to-long wavelength sensitivity of *Columba livia*'s double cones, a species with a similar visual system (Ödeen et al. 2011;

Ligon et al. 2018) and whose colour sensitivity has been documented (Hart 2001). This representation should be interpreted as a proxy for bird-of-paradise luminance perception rather than a quantitative estimate of double-cone stimulation. Importantly, varying the chosen RGB weights did not affect our results.

To simulate the bird's perception of a displaying individual at different distances (**Figure 1**), we filtered the images with a Fourier low-pass filter, using the known visual acuities of the common blackbird (*Turdus merula*) (Caves et al. 2024), a species that represents a good approximation of Victoria's riflebird visual acuity due to their similar body size and phylogenetic proximity, which broadly correlate with visual acuity. Note that cameras' distances to the display perch and fields of view, which are reported in the image metadata file available in the GitHub repository of the project, were accounted for by estimating the pixel size of each analysed image.

Individual birds were manually segmented with the Adobe Photoshop program (https://www.adobe.com/products/photoshop.html) to separate them from the background. JSON files were then created with the bird coordinates, and visual metrics were measured on both the bird's plumage and its background on images rendered to simulate different distances. Measures from the bird's plumage were compared to those of its background, and measures from adults to those of juveniles. The following metrics were computed separately for each region of interest (i.e. the bird's plumage and the background): mean pixel intensity, Shannon's entropy, and RMS contrast. Finally, the circularity of the display ovoid shape was estimated with a circularity index.

The mean pixel intensity was computed as the average of all pixel values for each region (plumage or background) independently.

Shannon's entropy (*H*) quantifies the randomness in the pixel values of an image, where higher entropy values correspond to images with more detail and complexity (Sanderson et al. 2025). If the entropy value for bird plumage is smaller than its background, resulting in a higher entropy difference between both regions, the detection of the bird should be improved. Shannon's entropy (H) was computed as:

$$H(X) = -\sum_{x \epsilon X} \quad p(x) log_2 p(x),$$

where *p(x)* is the probability of each pixel value (i.e., the likelihood for a specific intensity to occur at a pixel position in the image) and is defined as the number of pixels with intensity *x* divided by total number of pixels in the region.

To account for paired comparisons, we are reporting the difference in contrast values between plumage and background for each distance. The root-mean-square (RMS) contrast, or foreground–background contrast, was quantified as the absolute difference in mean luminance between plumage and background, normalised by the background luminance variability, defined as the standard deviation of the background pixel intensities. Higher values indicate greater visual contrast.

$$RMS = \frac{abs(\mu_{plumage} - \mu_{background})}{\sigma_{background}}$$

with $\mu_{plumage}$ and $\mu_{background}$ representing the average luminance of the plumage and the background, respectively, and $\sigma_{background}$, the standard deviation of the background luminance.

To characterize the regularity of the ovoid display contour shape, the convex hull circularity index was computed:

$$C_{hull} = \frac{4 * \Pi * area_{hull}}{perimeter_{hull} * 2}$$

where $area_{hull}$ and $perimeter_{hull}$ were extracted after computing the convex hull of the plumage region, that is, the ovoid shape of the display, using the *convex_hull* function from the Shapely Python package (https://shapely.readthedocs.io/en/2.1.2/reference/shapely.convex_hull.html). $C_{hull} \in (0, 1]$, where 1 indicates a convex shape and a smoother outline.

Signalling geometry in Victoria's riflebird displays

To estimate the portion of the female's field of view (FOV) that is covered by a displaying male, we calculated the solid angle (Ω) subtended by the male's body. Solid angle was estimated as the area (A) of the male's body projected onto a sphere divided by the square of the distance (r) from the female's eye to the male ($\Omega = A/r^2$) (see **Figure 3C** from main text). Here, A (cm^2) represents the area of the displaying male's body when both wings are raised, and r (cm) is the distance between the perceiver's eye and the male. This calculation assumes that the male's body approximates a spherical cap and that the perceiver has a complete (360°) field of view. Although this overestimates the total female FOV and therefore underestimates the FOV covered by male wings, retinal field data of typical songbirds, such as the common startling (*Sturnus vulgaris*) suggest that a 360˚ FOV is a crude, though useful assumption for our purposes (Martin 1986; Tyrrell and Fernández-Juricic 2017). Nonetheless, our results will tend towards underestimating the total FOV covered, rendering our estimates conservative.

Given r and A, the angular extent of the male in the horizontal and vertical planes was estimated from the solid angle using the relationship between solid angle and the vertex angle of a cone:

$$\Omega = 2\pi(1 - cos\theta)$$

where θ is the half-angle of the cone in radians. Solving for θ gives:

$$\theta = arccos(1 - \frac{\Omega}{2\pi})$$

The angle was converted to degrees to provide a more intuitive estimate of the FOV covered by the displaying male. The geometric means of the total body surface area of adult males included 20 additionally sampled frames from camera trap video, and distances between the females' eyes and the male included 21 frames from 5 adult males. Distances and surface areas were measured with the ruler and surface area tools in the ImageJ software (Rueden et al. 2017) calibrated using checkerboards (2.4 mm checker size) at display perches.

Given the surface area of the male's body, close-range displays subtend an estimated solid angle of 7.75 steradians (sr) on the perceiver's field of view (FOV) when both wings are raised, framing the metallic blue throat patch in the centre (**Figure 3B**). Because a complete sphere subtends 4π sr (~12.57 sr), males cover an estimated 61.69 % of an observing female's FOV. In the horizontal and vertical planes, males therefore subtend ~207˚ on the female's FOV (**Figure 3C**, **D**). Assuming a blind area in the horizontal plane of a typical passerine eye (40˚) (Martin 1986; Martin 2017; Tyrrell and Fernández-Juricic 2017), ~65% of the females' horizontal FOV is covered when both wigs are raised.

To measure how long the females' FOV is maximally covered by the displaying male (i.e., when both wings are raised during the dynamic phase of display), we annotated one representative display opportunistically filmed in high speed (120fps) using a Canon 5D mark IV with a Canon EF 100-400mm f/4.5-5.6L IS II USM zoom lens using the Loopy video annotation program (http://loopb.io, Loopbio, GmbH, Austria). Total FOV coverage was annotated as the duration from the first frame when both wingtips were seen to be touching to the frame where they were seen to separate. Total FOV coverage lasted for mean ± SD = 0.0524 s ± 0.0134 seconds (N = 58 events).

Statistical analysis

As small sample sizes limit the statistical power of most tests and therefore their interpretation, we report effect sizes and their 95% confidence intervals to quantify the differences between variables. Effect sizes were calculated with the *effsize* package in R (Torchiano 2020) using Cohen's *d* formula:

$$d = \frac{\boldsymbol{\mu}_{sample\,1} - \boldsymbol{\mu}_{sample\,2}}{\sigma_{pooled}},$$

With

$$\sigma_{pooled} = \frac{\sigma_{sample\,1}2 * (N_{sample\,1} - 1) + \sigma_{sample\,2}2 * (N_{sample\,2} - 1)}{N_{sample\,1} + N_{sample\,2} - 2}$$

where $\boldsymbol{\mu}_{sample}$ and σ_{sample} correspond to the mean and standard deviation of either adult (e.g., $\boldsymbol{\mu}_{sample\,1}$) and immature males (e.g. $\boldsymbol{\mu}_{sample\,2}$) and N_{sample} corresponds to the sample size of individuals. Hedge's correction for small sample sizes was also applied by multiplying the Cohen's *d* value by $\frac{N_{sample\,1}-2}{N_{sample\,1}-1.25}$ for paired measures (intensity and entropy metrics) or by $\frac{N_{total}-3}{N_{total}-2.25}$ for unpaired measures (contrast and circularity metrics), where

N_{total} is the total size of the two groups being compared (N_{total} = $N_{sample\ 1}$ + $N_{sample\ 2}$). Unpaired comparisons were performed as samples were independent.

Results & Discussion

Male riflebirds create conspicuous "black holes"

Riflebird display behaviour involves contiguous wing-morphing or so-called "shapeshifting" postures (Scholes and Laman 2012), with the bright blue throat patch or yellow integument of the mouth framed in the centre. To investigate features of the display related to signal efficacy, we quantified three metrics of display conspicuousness.

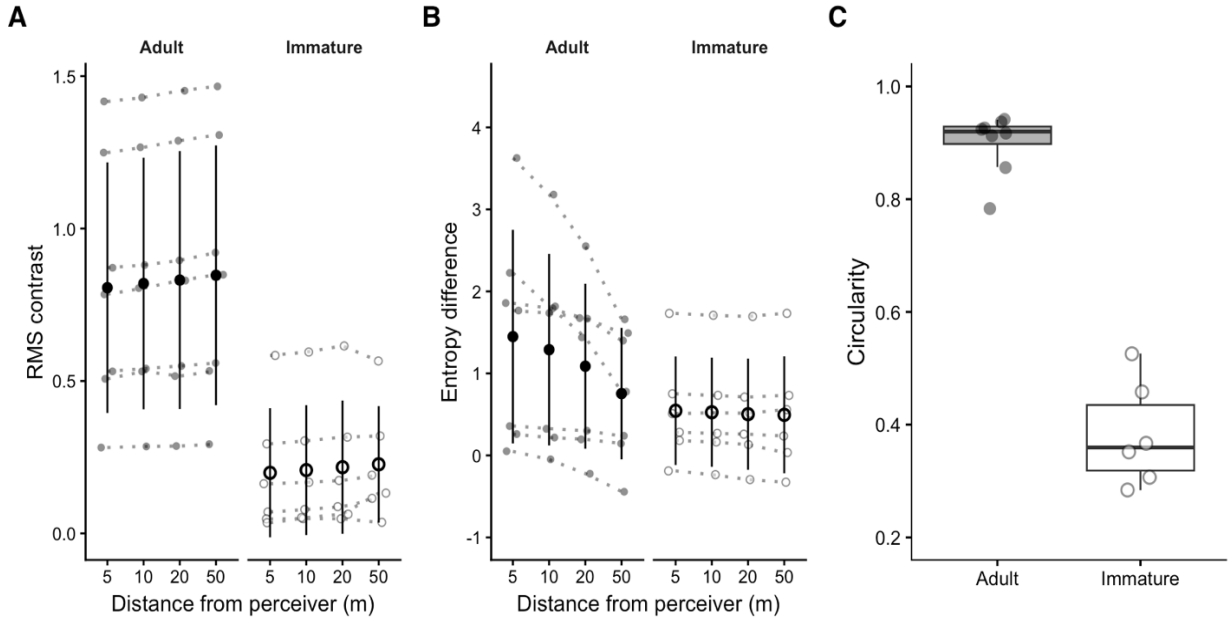

Figure 2. Root-mean-square (RMS) contrast between plumage and local background for adults and immatures across distances (from 5 to 50 m) (A). Plumage pattern complexity (Shannon entropy) plotted as the difference between backgrounds and adult and immature plumage across distances (B). Comparison of display pose circularity between immatures and adults (C). Points and error bars indicate mean ± standard deviations for each group, dotted lines join datapoints of same individuals across distances (A, B). Boxplots (C) show variation between individual birds (points) and show the median, upper and lower quartile, and interquartile range.

We first compared plumage pixel intensity of adult male displays to immature males with brown female-like plumage, relative to the background. We find that root-mean-square (RMS) contrast differed between age classes, where adults are much more detectable than immatures across distances (e.g., viewed from 5 m: d = 1.683, 95% CI: 0.359, 3.008 vs viewed from 50 m: d = 1.697, 95% CI: 0.369, 3.024) (**Figure 2A**). Unlike typical, brightly coloured colour patches used in courtship (Endler and Thery 1996; Uy and Endler 2004), this effect is driven by adult males being considerably darker than the visual background, creating an optical "black hole" effect against the cluttered rainforest backdrop. This interpretation contradicts the typical assumption that sexual selection should favour signal components that increase sensory stimulation relative to the environment, where signals that are brighter, louder, or more complex are expected to be the most attractive to a mate (Ryan and Cummings 2013). Nonetheless, in the initial formulation of sensory drive theory, Endler (1992) also predicted that, when given against intense background noise, selection may favour "weak" signals that create a sensory gap in the background, causing organisms to evolve dark colours with simple patterns to stand out from bright and complex backgrounds, respectively (Rowe et al. 2021).

Secondly, comparisons of pattern complexity difference between adult and immature male plumage and the background provide tentative evidence that adult males tend to contrast more with background pattern complexity (Shannon entropy of pixel intensities) than immatures, mostly at shorter viewing distances (e.g., at 5 m, d = 0.793, 95% CI: -0.390, 1.976; at 50 m; d = 0.316, 95% CI: -0.830, 1.462, **Figure 2B**). The lack of a stronger effect in

plumage complexity suggests that plumage intensity, rather than complexity, is a key feature related to signal efficacy. Pattern complexity is nonetheless an informative feature and suggests that structurally unmodified plumage may still significantly differ in pattern relative to the background.

Finally, quantification of the overall body shape indicates that morphological specialization of the flight feathers creates a more circular display posture in adult males (adults' circularity index is more than twice as high as immatures' (Circularity: $\bar{x}_{Adult} = 0.90$, $\bar{x}_{Immature} = 0.38$; $d = 6.83$, 95% CI: 4.91, 17.80; **Figure 2C**). These simpler and more clearly defined ovoid silhouettes are likely to be much more detectable to the vertebrate visual system compared to immature males (Bertamini et al. 2019). One reason is that visual signals that function to be highly detectable are expected to use high-contrast and sharply defined boundaries to exploit features of visual processing that enhance the perception of the target's outline (Troscianko et al. 2009; Egan et al. 2016). This feature is indeed what we find in male Victoria's riflebirds, which combine morphologically specialised, black plumage with a unique posture to create a highly conspicuous silhouette with a defined, circular outline. Together, these traits align with features predicted to enhance conspicuousness to vertebrate eyes when viewed from a distance.

Comparisons of both pixel intensity contrast (RMS contrast) and pattern complexity with the background and between age classes therefore suggest that riflebirds evolved simple, dark plumage as this enhances conspicuousness against the optically cluttered rainforest background.

Field of view effects of close-range displays

During dynamic displays, females view males up close by landing on the narrow display stump. **Figure 3** provides a series of photographs showing the typical relative positions of the male and female during the alternate wing-clap display (**Figure 3A, B**). To investigate key perceptual effects of this phase of the display, we combined geometric measurements and high-speed (120 fps) video. Basic size measurements show that feather-morphing displays of male Victoria's riflebirds create a large dish-shape that approximates the size of a dinner plate (geometric mean [GM] ≈ 650 cm2, diameter ≈ 30 cm). When this display is performed to a female on the display stump, the distance between the female's eye and the male's body is only ~10 cm (GM = 9.15 cm), resulting in males covering an estimated 61.69 % of an observing female's FOV, corresponding to a subtended angle of ~207˚ in horizontal and vertical planes (**Figure 3C, 3D**; see Materials and Methods). Assuming a blind area in the horizontal plane of a typical passerine eye (40˚) (Martin 1986; Tyrrell and Fernández-Juricic 2017), ~65% of the females' horizontal field of view (FOV) is covered when both wigs are raised. This full position is only held for 0.052 s ± 0.013 s (mean ± SD) (n = 58 events), resulting in brief, repetitive intervals where most of the females' FOV is occluded, temporarily creating a region of low sensory stimulation surrounding the blue throat patch (**Figure 3B**).

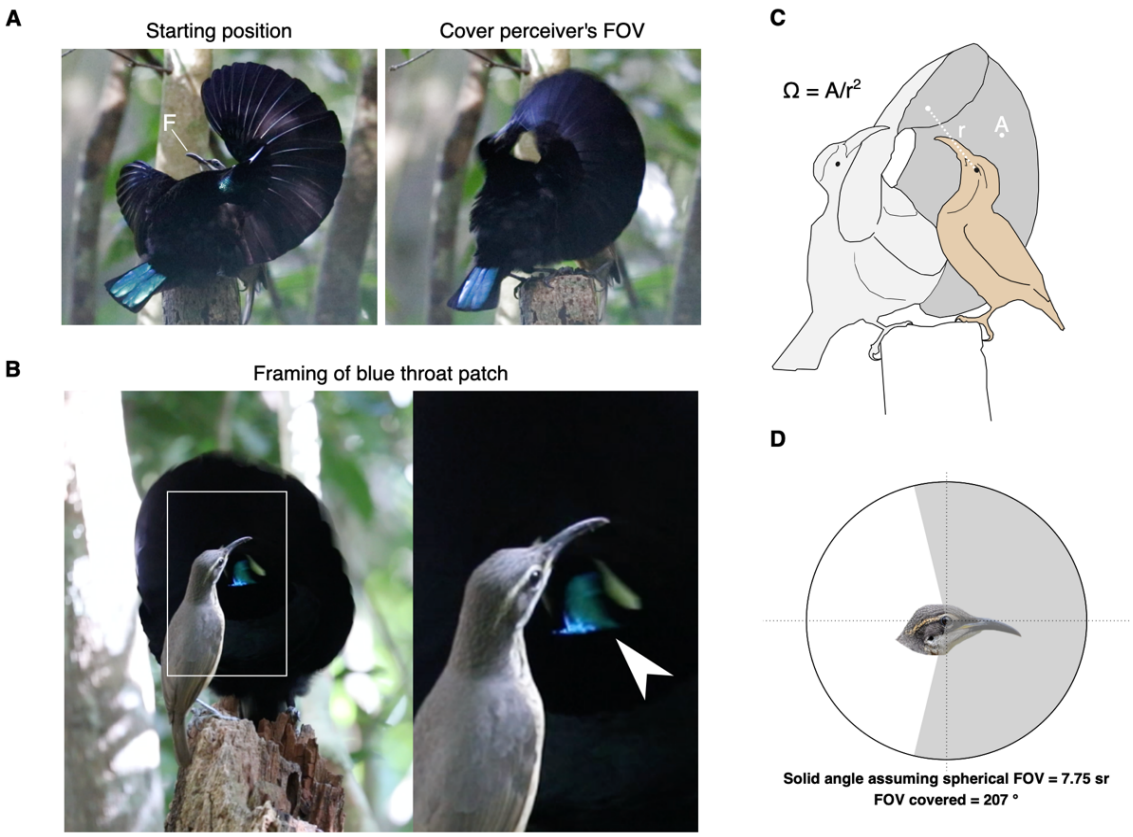

Figure 3. During dynamic displays, females view males up close (A). At close range, super-black plumage acts as a background for colour patches (B). Right panel: enlarged subsection of the male's body (indicated by the white box). The arrow shows the rapidly flashed blue throat patch. Colour patches are framed extremely quickly (~50 ms) during display by covering ~60% of the females' visual field (C). Vertical field of view (FOV) coverage with the covered region denoted in grey (D).

The geometric features of this close-range display could have several functions, including: (a) enhancing colour and luminance contrast with colour patches (McCoy et al. 2019; McCoy and Prum 2019), (b) creating the illusion of self-luminosity by preventing the estimation of ambient light intensity (McCoy et al. 2018), and (c) removing distractions in the visual background, thereby focusing female attention on colour patches (through high FOV coverage). Previous work within and beyond the bird-of-paradise family clearly shows that both colour and luminance contrast are enhanced when colour patches are spaced adjacent to extremely dark regions (McCoy et al. 2018; McCoy et al. 2019; McCoy and Prum

2019), though it is less clear whether this exploits a perceptual bias in colour constancy. Our current understanding of vertebrate vision renders all three hypotheses as plausible, suggesting they may act synergistically rather than being mutually exclusive.

Conclusion

Important insight into general patterns in biology can emerge from the study of extreme phenotypes (Clark et al. 2023). What can the unusual displays of birds-of-paradise teach us about signal evolution more broadly? Our results have several implications for the evolution of sexual signals.

First, regarding the evolution of complex colour patches, we show that sexual signals may not universally be selected to be bright or colourful so long as they maintain high conspicuousness, as predicted by Endler (1992). The circular-wings pose of male riflebirds is an excellent example of this, though there is more to these displays than high luminance contrast. When display features are selected for detectability, design features may be favoured that function as the inverse of disruptive colouration (Stevens and Cuthill 2006; Stevens and Merilaita 2009), where the body's outline is reinforced rather than broken up. This feature may be widespread in sexual signals or other forms of communication where detectability and conspicuousness are advantageous. This mechanism can improve detection by reinforcement of the body outline using monotone, high background-contrast colouration and a lack of disruptive marginal patterns, such as a simple border (Stevens and Merilaita 2009; Caves and Kelley 2023). These features may function principally by engaging edge-detection processing by receivers, creating a highly conspicuous body outline

(Stevens and Cuthill 2006). We could not directly test this with our image data, though it is likely that riflebird displays are particularly effective at stimulating edge-detection in female vision given their extreme luminance contrast and defined body outlines.

A second implication of this work is that the function of certain components of a courtship phenotype can change depending on the context in which they are viewed. In the case of riflebirds, black plumage creates both a conspicuous silhouette when viewed from a distance but also provides a high-contrast background for colour patches when viewed at close range. Although colour patches are also displayed at a distance, their small size likely means that they are much less effective at long range (they subtend a very small angle of the females' retina), and a background function does not explain why riflebird display poses are also extremely circular. Instead, the same signal components may be repurposed across stages of display to achieve different signal functions. Our geometric measurements suggest that, at close range, black plumage may function to blot out the female's FOV, creating a high-contrast background and potentially removing distractions in the environment (see above). This is comparable to the function of bowers in the bowerbirds, which control the female's visual perspective of male displays (Endler et al. 2010; MacGillavry, Frith, et al. 2025) and suggests that manipulation of receiver FOV may be a more widespread feature of elaborate visual signals.

Altogether, our study emphasises how taking the audience's perspective from a geometric point of view can illuminate key features of complex display behaviours. Given interspecific differences in visual acuity (Caves et al. 2018) and the configuration of the visual field (e.g., Martin 2017), the precise viewing geometries during complex displays likely represents an

important component of signal efficacy. The geometry of complex displays is therefore fruitful ground for research into the evolution of complex visual signals across diverse animals.

Data and script availability

All data and analysis scripts are made publicly available on the GitHub page of the research group (https://github.com/fusanilab). For complementary pattern analysis tools and pipelines, we invite the reader to also check the DEWPAT Python package (Sanderson et al. 2025).

References

Bertamini M, Palumbo L, Redies C. 2019. An advantage for smooth compared with angular contours in the speed of processing shape. Journal of Experimental Psychology: Human Perception and Performance. 45(10):1304–1318. https://doi.org/10.1037/xhp0000669

Caves EM, Brandley NC, Johnsen S. 2018. Visual Acuity and the Evolution of Signals. Trends in Ecology & Evolution. 33(5):358–372. https://doi.org/10.1016/j.tree.2018.03.001

Caves EM, Fernández-Juricic E, Kelley LA. 2024. Ecological and morphological correlates of visual acuity in birds. Journal of Experimental Biology. 227(2):jeb246063. https://doi.org/10.1242/jeb.246063

Caves EM, Kelley LA. 2023. Proportional processing of a visual mate choice signal in the green swordtail, *Xiphophorus hellerii*. Ecology Letters. 26(4):575–585. https://doi.org/10.1111/ele.14179

Clark CJ, Hutchinson JR, Garland T. 2023. The Inverse Krogh Principle: All Organisms Are Worthy of Study. Physiological and Biochemical Zoology. 96(1):1–16. https://doi.org/10.1086/721620

Cuthill IC et al. 2017. The biology of color. Science. 357(6350):eaan0221. https://doi.org/10.1126/science.aan0221

Echeverri SA et al. 2021. How Signaling Geometry Shapes the Efficacy and Evolution of Animal Communication Systems. Integrative and Comparative Biology. 61(3):787–813. https://doi.org/10.1093/icb/icab090

Echeverri SA, Morehouse NI, Zurek DB. 2017. Control of signaling alignment during the dynamic courtship display of a jumping spider Holman L, editor. Behavioral Ecology. 28(6):1445–1453. https://doi.org/10.1093/beheco/arx107

Egan J, Sharman RJ, Scott-Brown KC, Lovell PG. 2016. Edge enhancement improves disruptive camouflage by emphasising false edges and creating pictorial relief. Sci Rep. 6(1):38274. https://doi.org/10.1038/srep38274

Endler JA. 1992. Signals, Signal Conditions, and the Direction of Evolution. The American Naturalist. 139:S125–S153. https://doi.org/10.1086/285308

Endler JA, Endler LC, Doerr NR. 2010. Great Bowerbirds Create Theaters with Forced Perspective When Seen by Their Audience. Current Biology. 20(18):1679–1684. https://doi.org/10.1016/j.cub.2010.08.033

Endler JA, Gaburro J, Kelley LA. 2014. Visual effects in great bowerbird sexual displays and their implications for signal design. Proc R Soc B. 281(1783):20140235. https://doi.org/10.1098/rspb.2014.0235

Endler JA, Thery M. 1996. Interacting Effects of Lek Placement, Display Behavior, Ambient Light, and Color Patterns in Three Neotropical Forest-Dwelling Birds. The American Naturalist. 148(3):421–452. https://doi.org/10.1086/285934

Fleishman LJ, Prebish MGF, Leal M. 2020. The Effects of Limited Visual Acuity and Context on the Appearance of Anolis Lizard Dewlaps. Journal of Herpetology. 54(3) [accessed 2026 Feb 6]. https://bioone.org/journals/journal-of-herpetology/volume-54/issue-3/19-108/The-Effects-of-Limited-Visual-Acuity-and-Context-on-the/10.1670/19-108.full. https://doi.org/10.1670/19-108

Fleishman LJ, Yeo AI, Perez CW. 2017. Visual acuity and signal color pattern in an *Anolis* lizard. Journal of Experimental Biology. jeb.150458. https://doi.org/10.1242/jeb.150458

Frith CB, Cooper WT. 1996. Courtship Display and Mating of Victoria's Riflebird *Ptiloris victoriae* with Notes on the Courtship Displays of Congeneric Species. Emu - Austral Ornithology. 96(2):102–113. https://doi.org/10.1071/MU9960102

Hart NS. 2001. The Visual Ecology of Avian Photoreceptors. Progress in Retinal and Eye Research. 20(5):675–703. https://doi.org/10.1016/S1350-9462(01)00009-X

Kelley LA, Endler JA. 2012. Illusions Promote Mating Success in Great Bowerbirds. Science. 335(6066):335–338. https://doi.org/10.1126/science.1212443

Ligon RA et al. 2018. Evolution of correlated complexity in the radically different courtship signals of birds-of-paradise Price T, editor. PLoS Biol. 16(11):e2006962. https://doi.org/10.1371/journal.pbio.2006962

MacGillavry T. 2025. Contingency, Determinism, and Constraint in the Evolution of Elaborate Courtship Phenotypes. Evolution. qpaf064. https://doi.org/10.1093/evolut/qpaf064

MacGillavry T, Frith CB, Fusani L. 2024. The mechanics of male courtship display behaviour in the *Ptiloris* riflebirds (Aves: Paradisaeidae). Biological Journal of the Linnean Society. 143(1):blae077. https://doi.org/10.1093/biolinnean/blae077

MacGillavry T, Frith CB, Knoester J, Fusani L. 2025. The origins and functions of bowers in the bowerbirds: a review and synthesis. Emu - Austral Ornithology. [published online ahead of print]

MacGillavry T, Jadoul Y, Fusani L. 2025. Dancing male riflebirds create a dynamic sensory trajectory that guides female choice. Current Biology. 35:1–9. https://doi.org/DOI:%2010.1016/j.cub.2025.09.009

Martin GR. 1986. The eye of a passeriform bird, the European starling (Sturnus vulgaris): eye movement amplitude, visual fields and schematic optics. J Comp Physiol. 159(4):545–557. https://doi.org/10.1007/BF00604174

Martin GR. 2017. The Sensory Ecology of Birds. Oxford University Press. (Oxford Avian Biology).

McCoy DE et al. 2019. Structurally assisted super black in colourful peacock spiders. Proc R Soc B. 286(1902):20190589. https://doi.org/10.1098/rspb.2019.0589

McCoy DE, Feo T, Harvey TA, Prum RO. 2018. Structural absorption by barbule microstructures of super black bird of paradise feathers. Nat Commun. 9(1):1. https://doi.org/10.1038/s41467-017-02088-w

McCoy DE, Prum RO. 2019. Convergent evolution of super black plumage near bright color in 15 bird families. Journal of Experimental Biology. 222(18):jeb208140. https://doi.org/10.1242/jeb.208140

Ödeen A, Håstad O, Alström P. 2011. Evolution of ultraviolet vision in the largest avian radiation - the passerines. BMC Evol Biol. 11(1):313. https://doi.org/10.1186/1471-2148-11-313

Oliveros CH et al. 2019. Earth history and the passerine superradiation. Proc Natl Acad Sci USA. 116(16):7916–7925. https://doi.org/10.1073/pnas.1813206116

Rowe ZW et al. 2021. Background complexity can mitigate poor camouflage. Proc R Soc B. 288(1963):20212029. https://doi.org/10.1098/rspb.2021.2029

Rueden CT et al. 2017. ImageJ2: ImageJ for the next generation of scientific image data. BMC Bioinformatics. 18(1):529. https://doi.org/10.1186/s12859-017-1934-z

Ryan MJ, Cummings ME. 2013. Perceptual Biases and Mate Choice. Annu Rev Ecol Evol Syst. 44(1):437–459. https://doi.org/10.1146/annurev-ecolsys-110512-135901

Sanderson JA, Aumentado-Armstrong T, Dufresne-Camaro C, Mahler DL. 2025. Dude, everyone wants pattern analysis tools (DEWPAT): Tools for measuring visual pattern complexity from digital images. Methods Ecol Evol. 16(6):1095–1105. https://doi.org/10.1111/2041-210X.70048

Santacà M, Quigley C, Fusani L. 2025. Circles of deception: the Ebbinghaus illusion from fish to birds. Front Psychol. 16:1653695. https://doi.org/10.3389/fpsyg.2025.1653695

Scholes E, Laman T. 2012. Birds of Paradise: Revealing the World's Most Extraordinary Birds. National Geographic Society.

Stevens M, Cuthill IC. 2006. Disruptive coloration, crypsis and edge detection in early visual processing. Proc R Soc B. 273(1598):2141–2147. https://doi.org/10.1098/rspb.2006.3556

Stevens M, Merilaita S. 2009. Defining disruptive coloration and distinguishing its functions. Phil Trans R Soc B. 364(1516):481–488. https://doi.org/10.1098/rstb.2008.0216

Torchiano M. 2020. Package 'effsize'. https://github.com/mtorchiano/effsize/

Troscianko T et al. 2009. Camouflage and visual perception. Phil Trans R Soc B. 364(1516):449–461. https://doi.org/10.1098/rstb.2008.0218

Tyrrell LP, Fernández-Juricic E. 2017. The Hawk-Eyed Songbird: Retinal Morphology, Eye Shape, and Visual Fields of an Aerial Insectivore. The American Naturalist. 189(6):709–717. https://doi.org/10.1086/691404

Uy JAC, Endler JA. 2004. Modification of the visual background increases the conspicuousness of golden-collared manakin displays. Behavioral Ecology. 15(6):1003–1010. https://doi.org/10.1093/beheco/arh106

Yorzinski JL et al. 2013. Through their eyes: selective attention in peahens during courtship. Journal of Experimental Biology. 216(16):3035–3046. https://doi.org/10.1242/jeb.087338